ELSEVIER

Biochimica et Biophysica Acta 1467 (2000) 198–206

BIOCHIMICA ET BIOPHYSICA ACTA
BBA

www.elsevier.com/locate/bba

Order–disorder transition in bilayers of diphytanoyl phosphatidylcholine

W.C. Hung [a], F.Y. Chen [a], Huey W. Huang [b,*]

[a] *Department of Physics, National Central University, Chung-Li 32054, Taiwan*
[b] *Department of Physics, Rice University, Houston, TX 77251, USA*

Received 19 January 2000; received in revised form 7 March 2000; accepted 13 April 2000

Abstract

A comparative study on bilayers of diphytanoyl phosphatidylcholine (DPhPC) and bilayers of dimyristoyl phosphatidylcholine (DMPC) was made by X-ray lamellar diffraction as a function of temperature and the degree of hydration. An order–disorder phase transition of DPhPC reveals an interesting contrast to the standard model of DMPC. Electron density profiles allow us to deduce the conformational changes which occur in the headgroup-glycerol region and in the chain region. The important conclusion is that the lipid headgroup may have different conformational energetics in lipids of different chains. We explain why this is important to protein–membrane interactions.

Keywords: Diphytanoyl phosphatidylcholine bilayer; Dimyristoyl phosphatidylcholine; X-ray diffraction; Phase transition; Headgroup energetics; Chain energetics

1. Introduction

Diphytanoyl (3,7,11,15-tetramethylhexadecanoic) phosphatidylcholine (DPhPC) forms excellent model bilayers [1]. It is one of the commonly used lipids in electrophysiological measurements [2] and in experiments of peptide–lipid interactions [3–10]. However, while other model lipids, such as dimyristoyl phosphatidylcholine (DMPC), have been extensively studied, very little is known about the physical properties of DPhPC. In this paper, we will use X-ray diffraction to investigate an order–disorder transition exhibited by DPhPC bilayers. We will show that DPhPC has unusual properties compared with more commonly known phospholipids, such as DMPC.

Biological membranes are a mixture of lipids (and proteins), and contain both saturated and unsaturated chains. To imitate the chain disorder in native membranes, lipids of unsaturated chains, such as dioleoyl phosphatidylcholine or palmitoyloleoyl phosphatidylcholine, are often used to form model bilayers. DPhPC has the advantage of being composed of hydrocarbon chains with saturated bonds, therefore is more stable. The presence of methyl groups at regular intervals along the acyl chains causes the *trans* and one of *gauche* rotamers to be nearly energetically equivalent [11]. The steric re-

Abbreviations: DPhPC, diphytanoyl phosphatidylcholine; DMPC, dimyristoyl phosphatidylcholine; PC, phosphatidylcholine; PE, phosphatidylethanolamine; P/L, peptide to lipid molar ratio; RH, relative humidity; PtP, the phosphate-to-phosphate distance across the lipid bilayer; D_c, the thickness of the hydrophobic region

* Corresponding author. Fax: +1-713-348-4150;
E-mail: hwhuang@rice.edu

0005-2736/00/$ – see front matter
PII: S0005-2736(00)00221-2

quirements of the methyl branches clearly prevent efficient lateral packing of the acyl chains, resulting in considerable disorders in the chain configurations.

The chain configuration is closely related to the cross sectional area of the lipid. One key parameter in peptide–lipid interactions is the areal ratio of the headgroup to the chains: A_{hg}/A_{ch}. It has been shown that membrane active peptides, such as alamethicin [3–5], magainin [6,7], protegrin [8,9] and melittin [10] can bind to a lipid bilayer in two distinct states. At low peptide-to-lipid ratio (P/L), the peptides tend to adsorb in the headgroup region. However, when P/L exceeds a lipid-dependent threshold value P/L*, the peptides tend to insert transmembrane. The threshold P/L* clearly depends on the A_{hg}/A_{ch} of the lipid. For example, lipids with straight chains, such as DMPC, have relatively large A_{hg}/A_{ch}. Within the observable range of P/L, alamethicin is always inserted transmembrane. This can be qualitatively understood as the bilayer having little room in the headgroup region to accommodate peptides. DOPC has a smaller A_{hg}/A_{ch} compared with DMPC, so there is some room in the headgroup region. Experiment showed that alamethicin adsorbs in the headgroup region of DOPC bilayers until P/L exceeds P/L* $\sim$1/200 [3]. DPhPC has an even smaller A_{hg}/A_{ch}, so it can accommodate alamethicin in the headgroup region until P/L exceeds P/L* $\sim$1/40 [4,12]. We can further decrease the average A_{hg}/A_{ch} by using the mixtures of DPhPC and diphytanoyl phosphatidylethanolamine (DPhPE), because the headgroup PE is smaller than PC. As expected, we found that in the PC/PE mixtures, P/L* increased progressively with the amount of PE [12].

Thus DPhPC happens to be an ideal lipid for studying peptide–lipid interactions. Its A_{hg}/A_{ch} gives rise to experimentally convenient threshold values P/L* that allow us to investigate both the surface state and inserted state of peptides. The result presented in this paper reveals interesting lipid energetics and its consequences on A_{hg}/A_{ch}.

2. Materials and method

2.1. Materials

Diphytanoyl phosphatidylcholine (DPhPC) and dimyristoyl phosphatidylcholine (DMPC), were purchased from Avanti Polar Lipids (Alabaster, AL) and used without further purification. Oriented multilayer samples were prepared by a method described previously [7]. Lipid was dissolved in 1:1 methanol/chloroform solvent. Five milligrams of lipid was deposited evenly on a clean microscope slide to an area approximately 15×15 mm^2. Once the sample appeared dry, it was placed in vacuum to ensure the complete removal of the solvent. The samples were then equilibrated in a humidity chamber. Before the X-ray measurement, the oriented sample was inspected by using a polarized microscope for its quality of alignment [13].

2.2. Method

X-ray diffraction was measured by θ-2θ scan with Cu K_α radiation generated at 30 kV–30 mA. The plane of the lipid multilayers was oriented vertical. Each scan covered θ from 0.5° to 13° with step size 0.005°, 1 s per step. The humidity/temperature chamber enclosed the goniometer head and was insulated from room temperature. The temperature of the sample was monitored by a Pt-100 thermoresistor and controlled to 0.025°C via a computer-based, feedback system. The chamber was connected to a water source whose temperature was adjusted to vary the relative humidity in the immediate vicinity of the lipid sample. A combined thermometer and hygrometer (accuracy 0.1°C and 0.1% RH for RH $<\sim$98%, respectively) was positioned next to the sample. The measured vapor temperature T_v and relative humidity RH_v were used to calculate the relative humidity for the sample $RH = RH_v \times$(saturated vapor pressure at T_v/saturated vapor pressure at the sample temperature T). The osmotic pressure Π is defined as $\Pi = -(k_B T/v_w)\times\ln(RH)$, where k_B is the Boltzmann constant and v_w the volume of a single water molecule. For each humidity setting, the sample was equilibrated for at least 6 h, before X-ray scan. The equilibrium was confirmed by at least three consecutive unchanging diffraction patterns. No radiation damage was detected by thin layer chromatography or change of diffraction pattern in the same condition. Representative diffraction patterns are shown in Fig. 1.

Data reduction was straightforward [14], and has

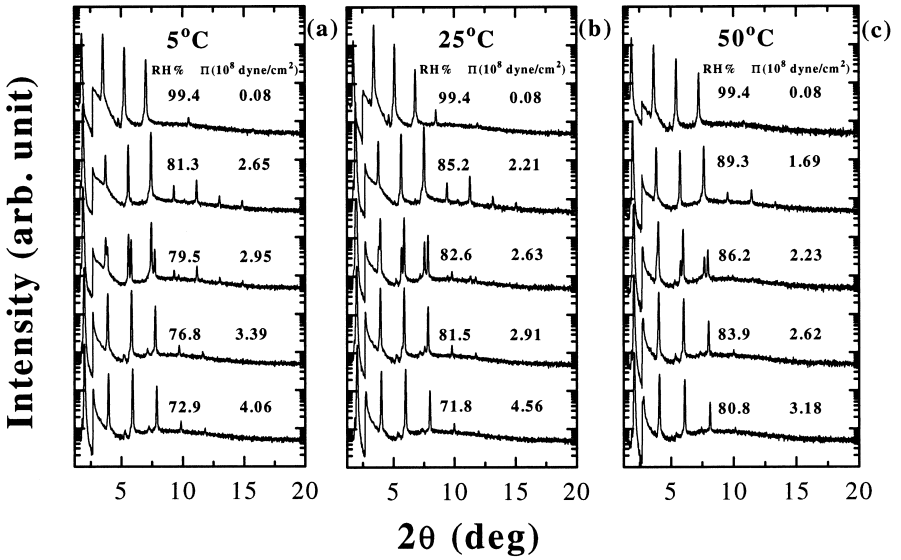

Fig. 1. Diffraction patterns along three isotherms: (a) $T=5$°C; (b) $T=25$°C; and (c) $T=50$°C. At low Π values (high degrees of hydration), each pattern shows a single lamellar series. DPhPC is in the L_α phase. Within a small range of Π (or RH), the patterns show two lamellar series (the middle pattern of each panel), indicating that there are two lamellar phases in coexistence. Upon further dehydration, the patterns became single lamellar series again. DPhPC is now in the L_α' phase.

been described in detail in previous membrane diffraction papers [4,15,16]. Briefly, the procedure included background subtraction, corrections for absorption and diffraction volume, and, after integration for each Bragg peak, corrections for polarization and the Lorentz factor. The reduction resulted in the relative diffraction intensities $|F(2\pi h/D)|^2$ ($h=1, 2, \ldots$). The phases of the diffraction amplitude $F(2\pi h/D)$ were determined by the swelling method [17,18] where the diffraction amplitudes of different D values (measured at different hydration levels) were demanded to fall on a single smooth curve (Fig. 2). With the phases determined, the relative diffraction amplitudes were Fourier transformed to obtain the unnormalized electron density profile $\rho=\Sigma_h F(2\pi h/D)\cos(2\pi hz/D)$. ρ is related to the true electron density profile ρ_o by $\rho=b\rho_o+c$, where b and c are constants. For our present purpose, normalization is unnecessary [15].

3. Results and discussion

In order to appreciate the unusual properties of DPhPC, we will make a direct comparison with DMPC which is often regarded as a representative phospholipid. The data of DMPC has been described in another paper [19]. They are included here alongside DPhPC for the purpose of comparison.

3.1. Phase diagrams

As shown in Fig. 1, when DPhPC sample was progressively dehydrated along an isotherm, there is a range of Π in which the diffraction pattern consists of two lamellar series, indicating two lamellar phases in coexistence. This phase transition was first discov-

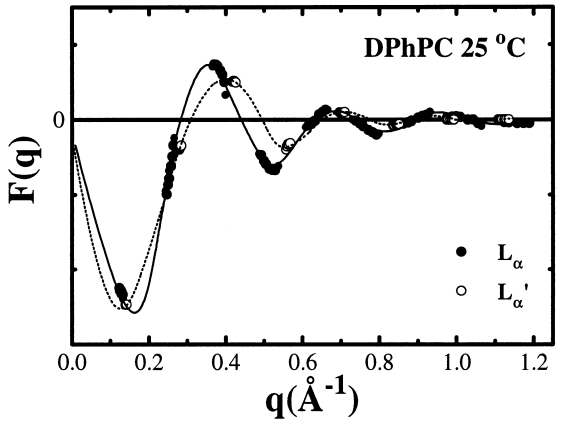

Fig. 2. Phasing diagram by the swelling method. Diffraction amplitudes $F(q)$ of different D values fall on a single smooth curve. $q=2\pi h/D$, ($h=1, 2, 3, \ldots$). The $F(q)$ values of the two phases are distinctly different.

ered by Wu et al. [4]. The transition is unlike the well-known main transition of DMPC where the hydrocarbon chains transform from disordered fluid configurations into the all *trans* configuration. Such transitions are characterized by a change of a wide angle band (at $\theta \sim 10°$) into sharp peaks [4,20]. No such change in the wide angle band was observed in the transition of DPhPC [4]. Other possible phase changes have been reported by NMR studies of DPhPC in powder samples, including possible hexagonal and isotropic phases [21]. It is possible that under our experimental condition, the potential barrier for a transition to a hexagonal or an isotropic phase is too high, so the latter were not observed.

Fig. 3 shows the Π–T phase diagram of DPhPC in comparison with that of DMPC. We call the phase including the full hydration the L_α phase and the phase in the lower hydration the L_α' phase. Note the important difference in the slope of the phase boundary of DPhPC versus that in DMPC. In DMPC, the dry phase corresponds to the low temperature gel phase ($L_{\beta'}$ and the rippled $P_{\beta'}$). That means that as the lipid is dehydrated along an isotherm, it transforms from a disordered phase into an ordered phase. In contrast, the dry phase of DPhPC corresponds to the high temperature phase. According to thermodynamics, a phase change by increasing temperature brings a system from an ordered phase to a disordered phase. Thus we conclude from the phase diagram that the L_α' phase is the disordered phase relative to the L_α phase. The dehydration transition along an isotherm is an order-to-disorder phase transition, exactly opposite to DMPC.

This can be explicitly shown as follows. Denote the Gibbs free energy of the bilayer/water system by G. At constant (atmospheric) pressure, we have $dG = -SdT + \mu_l dN_l + \mu_w dN_w$, where S is the entropy of the system, μ_l and N_l are the chemical potential and the number of lipid molecules, respectively, and μ_w and N_w are the chemical potential and the number of water molecules, respectively. By the Euler relation $G = \mu_l N_l + \mu_w N_w$, we obtain the Gibbs–Duhem relation

$$d\mu_l = -\left[\frac{S}{N_l}\right]dT - \left[\frac{N_w}{N_l}\right]d\mu_w = -\left[\frac{S}{N_l}\right]dT + \left[\frac{V_w}{N_l}\right]d\Pi \quad (1)$$

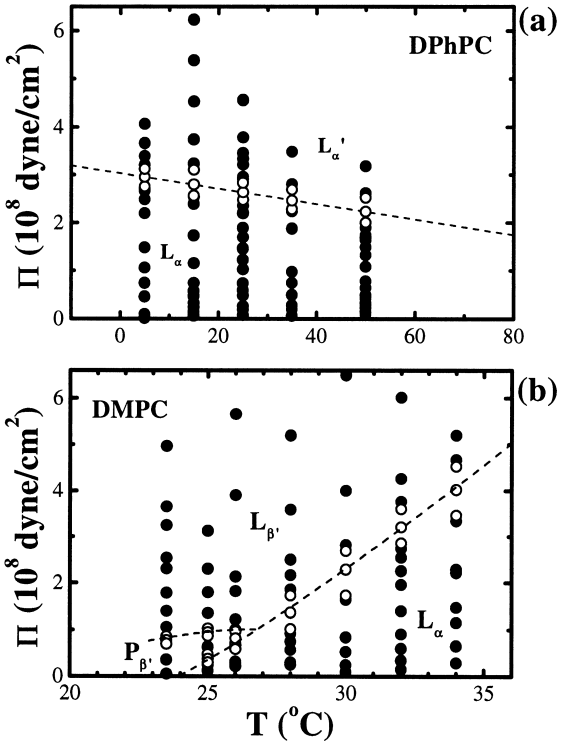

Fig. 3. Π–T phase diagrams of DPhPC (a) in comparison with DMPC (b). Diffraction patterns were recorded at every point shown in the phase diagrams. The open circles are where we recorded two distinct lamellar series in the diffraction pattern, indicating two phases in coexistence. A more detailed phase diagram of DMPC is shown in reference [19]. The dashed lines indicate the phase boundaries.

The last equation is obtained by the definition of osmotic pressure Π: $\mu_w = \mu_o - V_w\Pi$, where μ_o is the chemical potential of bulk water and V_w is the volume of water associated with lipid. The quantities in square brackets are normalized to per lipid molecule. From Eq. 1, one obtains the Clausius–Clapeyron equation [22].

$$\left(\frac{d\Pi}{dT}\right)_{ph.bd.} = \frac{[S/N_l] - [S/N_l]'}{[V_w/N_l] - [V_w/N_l]'}. \quad (2)$$

This derivation is similar to Leikin et al. [23]. The derivative $(d\Pi/dT)_{ph.bd.}$ is taken along the phase boundary. Let the unprimed quantities denote the hydrated phase and primed quantities the dehydrated phase. Then the denominator is positive in all cases. For DMPC, $(d\Pi/dT)_{ph.bd.}$ is positive. Therefore, $[S/N_l] > [S/N_l]'$, i.e. the dehydrated phase (primed) has lower entropy or is more ordered. For DPhPC, ($d\Pi$/

$dT)_{ph.bd.}$ is negative, so $[S/N_l] > [S/N_l]'$. The dehydrated phase has higher entropy and is more disordered.

In an earlier study by Lindsey et al. [11], DPhPC in water was investigated with differential thermal analysis from −120° to +120°C, and it was concluded that the lipid may have only one phase. The absence of a phase transition from −120° to +120°C (in full hydration) is consistent with our phase diagram Fig. 3. However, our phase diagram indicates a possibility of a phase transition in full hydration at a higher temperature, perhaps ∼200°C.

3.2. Electron density profiles

Let us briefly review DMPC first ([19] and references therein, [24]). As shown in Fig. 4, the electron density profiles have the conventional feature for a bilayer structure: a main peak for the phosphate group and a plateau for the double-chain methylenes on each side of the bilayer and a central trough for the methyl terminals. In addition, the electron density profiles in the gel ($L_{\beta'}$) phase show a pair of distinct secondary peaks on the inside of the main peaks. The separation between the main and the secondary peaks I_h is constant at 4.85 Å despite variations of D. In another paper [19], we have shown that the same peak separation was found in dilauroyl phosphatidylcholine (DLPC) and even extended to the fluid phase in low hydration. By a careful comparison with in-plane diffraction [25,32] and crystallographical data [26,27], we have identified the secondary peak as the position of the interfacial atoms C3-C2-O21-C21-C22 of the β-chain, which is bent in a L-shape (see Fig. 5). The PC-glycerol region is the same as the crystal structure throughout the hydration range. The same PC-glycerol structure is maintained in the fluid phase, except that there are some fluctuations, particularly near the full hydration [19,28,29].

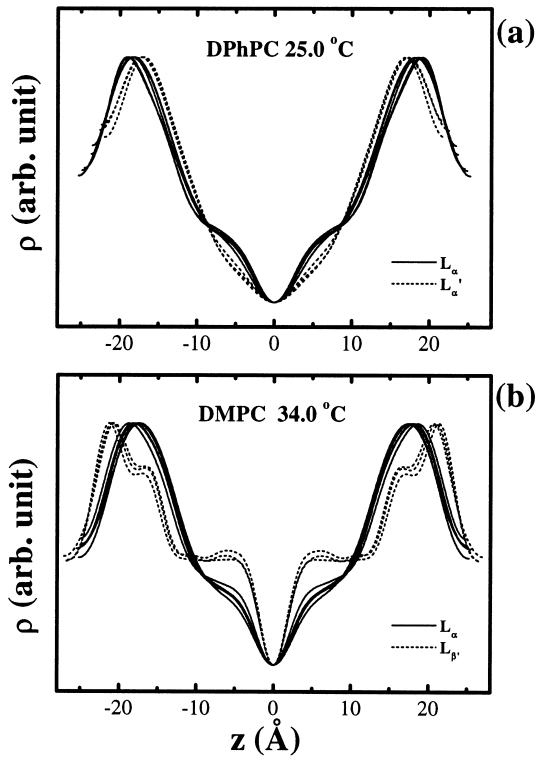

Fig. 4. Electron density profiles of DPhPC (a) and DMPC (b). Each panel shows a series of electron density profiles at different degrees of hydration along an isotherm (see Fig. 3). Each phase has its own characteristic profile.

Accordingly, the two chains of DMPC are not equivalent: the β-chain has one 90° bend and the γ-chain is straight [30]. The shape of the central trough in the electron density profile reflects these unequal extensions. The phosphate-to-phosphate distance (PtP) includes the invariant headgroup thickness I_h and the hydrophobic thickness D_c: $PtP = 2I_h + D_c$. This commonly accepted model for DMPC is depicted in Fig. 5 [24]. In the gel phase, the variation of D_c is due to the changes in the chain tilt angle. In the fluid phase, the variation of D_c is due to different degrees of *trans−gauche* excitations. In both cases, the variation in PtP is due to the variation in D_c. The chain area A_{ch} is inversely proportional to D_c*(i.e., $A_{ch} \cdot D_c$ = hydrocarbon volume ≈ constant), whereas the headgroup area A_{hg} is constant because of the invariant I_h. Thus the variation of the parameter A_{hg}/A_{ch} is essentially the result of the chain dynamics.

We now compare the electron density profiles of DPhPC with DMPC (Fig. 4). In the L_α phase, the profiles of DPhPC are similar to DMPC indicating similar chain configurations. However in the L_α' phase, the trough becomes rounded, indicating a change in chain configurations.

3.3. Molecular model

To gain further insight, we examine the D vs. Π

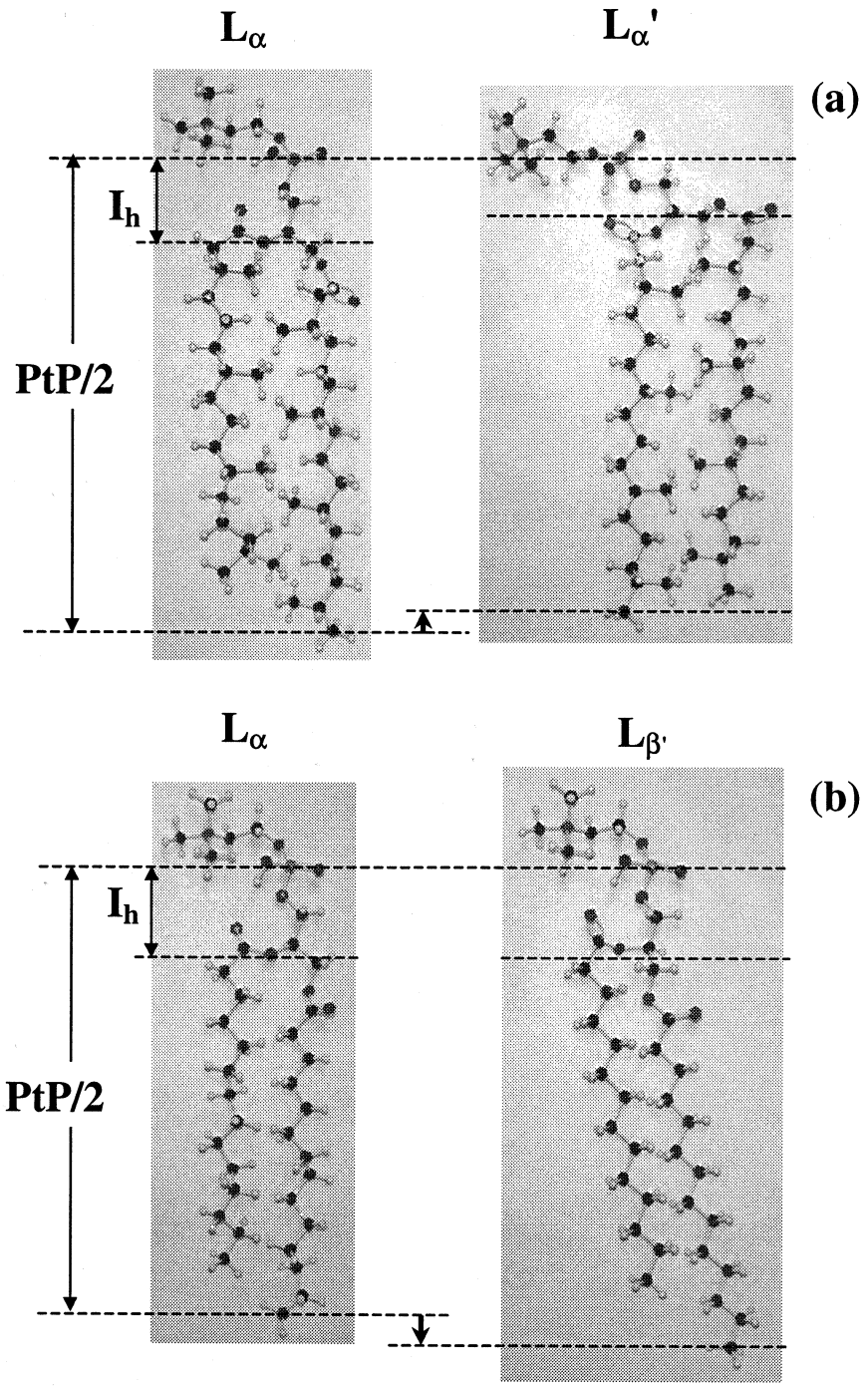

Fig. 5. Molecular models of DPhPC and DMPC. (a) represents the proposed model for DPhPC described in the text. (b) represents the commonly accepted model for DMPC [24]. The β chain is on the left and the γ chain on the right.

and PtP vs. Π curves (Fig. 6). At the dehydration transition of DMPC, PtP undergoes a ∼4 Å increase (δPtP∼4 Å) that has been understood as the result of chain straightening [24]. At the same time D increases ∼2 Å, $\delta D \sim 2$ Å. The volume of water associated with each lipid molecule is $[V_w/N_l] = \frac{1}{2} D \cdot A_{ch} - V_l$, where V_l is the volume of the lipid molecule which, like the hydrocarbon volume, can be regarded as a constant in a first-order approximation. Thus the change of water volume

$\delta[V_w/N_l] = \frac{1}{2}\delta(D{\cdot}A_{ch})$. The simplest way to see the sign of the water volume change is to examine

$$\frac{\delta(D{\cdot}A_{ch})}{(D{\cdot}A_{ch})} = \frac{\delta D}{D} + \frac{\delta A_{ch}}{A_{ch}} = \frac{\delta D}{D} - \frac{\delta D_c}{D_c}. \quad (3)$$

For DMPC, the headgroup-glycerol structure is invariant, so we have $\delta D_c = \delta PtP > \delta D$. Together with $D > D_c$, it is easy to see that Eq. 3 is negative, as it should be for a dehydration transition.

As we see in Fig. 6, the transitional changes in DPhPC is opposite to DMPC in both D and PtP. Therefore, the transition of DPhPC must be fundamentally different from what happens in DMPC. We propose to explain DPhPC by the model depicted in Fig. 5. First, in the L_α phase: its electron density profiles are similar to DMPC. We assume that the molecular configuration of DPhPC is similar to DMPC: the glycerol backbone is normal to the bilayer, the γ-chain is straight, and the β-chain is bent. Of course, in the high hydration region, both chains are disordered by *trans–gauche* excitations, but we believe that right before the dehydration transition the two chains are arranged as shown in Fig. 5 in which the two chains are packed in a space-saving fashion like two combs inserting into each other. The methyl branches are staggered in the order of 3,3′,7,7′,11,11′,15,15′, where unprimed methyl branches are that of the β-chain and the primed methyl branches are that of the γ-chain. The largest PtP is attained at this point on the Π coordinate, so we believe that the chains are maximally extended in such a packing configuration. The longer extension by the γ-chain, relative to the β-chain, gives rise to the sharp central trough in the electron density profile, similar to DMPC in its L_α phase.

Upon transition to the L_α' phase, three changes occur: (1) the central trough becomes rounded; (2) PtP decreases by ∼4 Å, ($\delta PtP \sim -4$ Å); and (3) D decreases by ∼2 Å, ($\delta D \sim -2$ Å). Let us suppose that like in DMPC, the headgroup-glycerol structure is invariant. Then the situation is similar to DMPC, except that the signs of δD and δD_c are now both negative. Therefore Eq. 3 is positive, that is not allowed for a dehydration transition. Thus the first conclusion is that the headgroup-glycerol structure has to change on the transition.

We propose that the transition is achieved by moving the β-chain one notch down the γ-chain, so the methyl branches are now arranged in the order 3′,3,7′,7,11′,11,15′,15 (Fig. 5). This model qualita-

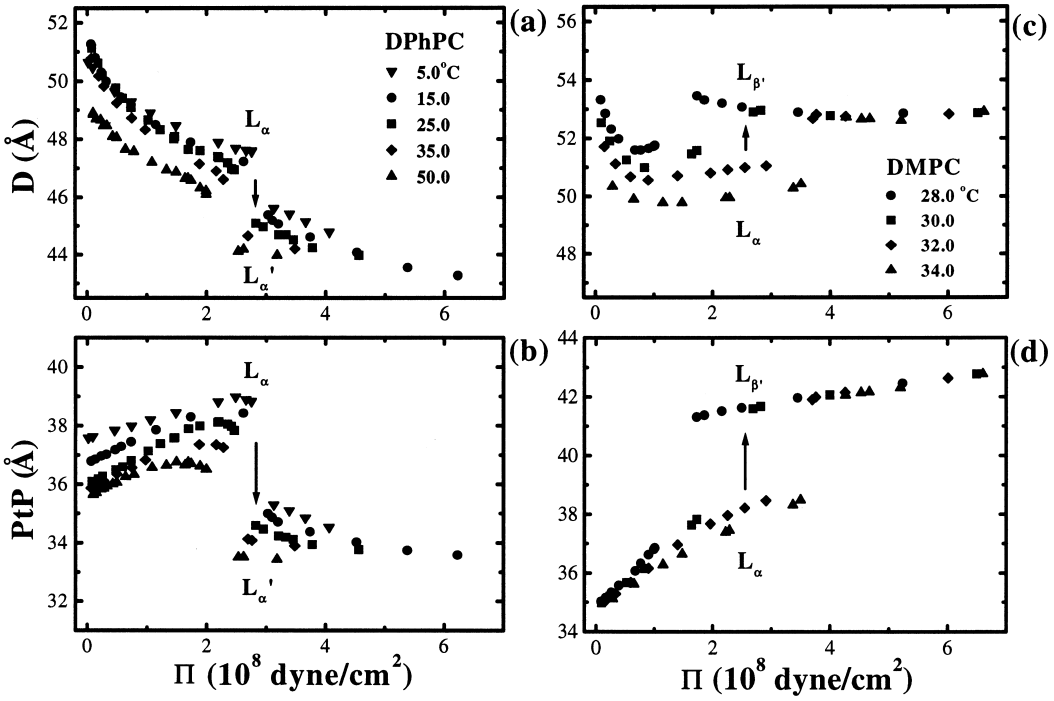

Fig. 6. D vs. Π and PtP vs. Π of DPhPC (a,b) in comparison with DMPC (c,d). The arrows indicate the dehydration transition.

tively explains the three changes observed above: (1) the smaller difference in the extensions of the two chains explains the roundedness of the central trough (Fig. 5); and (2) the new packing configuration of the two chains forces the glycerol backbone to tilt from the upright orientation. That would decrease the distance I_h from the phosphate to the edge of the hydrocarbon region, hence decrease both PtP and D.

The model presented above is qualitative. It provides a plausible explanation for the contrasting behavior of DPhPC relative to DMPC. At the moment there is no sufficient experimental information that would provide structural details for a more quantitative analysis. The most important implication of this analysis is that the lipid headgroup configuration may behave differently in lipids with different chains. If the above model is correct, the chain area A_{ch} is essentially constant in DPhPC bilayers. The variation of A_{hg}/A_{ch} with hydration (and possibly with other variables as well) is primarily governed by the energetics of the headgroup conformation rather than by that of the chains, exactly opposite to the case of DMPC.

4. Conclusion

The degree of hydration, like temperature, is not a normal physiological variable. However, we have found variation of hydration to be a usual experimental parameter for probing peptide–membrane interactions [3–10] as well as probing the physical properties of membranes [19]. For example, according to the phase diagram Fig. 3, one would need to go to a very high temperature ($\sim$200°C) to reach the order–disorder phase transition of DPhPC. By variation of hydration, we can study this transition in room temperature. More recently, we have also found that it is possible to crystallize supramolecular assemblies of peptides in membranes by variation of hydration [31].

The order–disorder transition reveals unusual conformational energetics of DPhPC. In particular, the energetics of the lipid headgroup configuration is entirely different from DMPC. This provides a caveat to the conventional use of DMPC as a standard model for bilayer membranes. The proposed molecular model for DPhPC provides a basis for analyzing protein–membrane interactions when DPhPC is used as a model membrane.

Acknowledgements

F.Y.C. was supported by the Department of Physics, National Central University and by National Science Council (Taiwan) through Contract NSC 87-2112-M-008-001. H.W.H. was supported by National Institutes of Health Grant GM55203 and by the Robert A. Welch Foundation.

References

[1] W.R. Redwood, F.R. Pefiffer, J.A. Weisbach, T.E. Thompson, Biochim. Biophys. Acta 233 (1971) 1–6.
[2] A.M. O'Connell, R.E. Koeppe, O.S. Andersen, Science 250 (1990) 1256–1259.
[3] H.W. Huang, Y. Wu, Biophys. J. 60 (1991) 1079–1087.
[4] Y. Wu, K. He, S.J. Ludtke, H.W. Huang, Biophys. J. 68 (1995) 2361–2369.
[5] K. He, S.J. Ludtke, W.T. Heller, H.W. Huang, Biophys. J. 71 (1996) 2669–2679.
[6] S.J. Ludtke, K. He, Y. Wu, H.W. Huang, Biochim. Biophys. Acta 1190 (1994) 181–184.
[7] S.J. Ludtke, K. He, H.W. Huang, Biochemistry 34 (1995) 16764–16769.
[8] W.T. Heller, A.J. Waring, R.I. Lehrer, H.W. Huang, Biochemistry 37 (1998) 17331–17338.
[9] W.T. Heller, A.J. Waring, R.I. Lehrer, T.A. Harroun, T.M. Weiss, L. Yang, H.W. Huang, Biochemistry 39 (2000) 139–145.
[10] T.A. Harroun, PhD thesis, Rice U. 1999.
[11] H. Lindsey, N.O. Petersen, S.I. Chan, Biochim. Biophys. Acta 555 (1979) 147–167.
[12] W.T. Heller, K. He, S.J. Ludtke, T.A. Harroun, H.W. Huang, Biophys. J. 73 (1997) 239–244.
[13] H.W. Huang, G.A. Olah, Biophys. J. 51 (1987) 989–992.
[14] B.E. Warren, X-ray Diffraction, Dover Publications, Mineola, New York, 1969, pp. 116–150.
[15] F.Y. Chen, W.C. Hung, H.W. Huang, Phys. Rev. Lett. 79 (1997) 4026–4029.
[16] G.A. Olah, H.W. Huang, W. Liu, Y. Wu, J. Mol. Biol. 218 (1991) 847–858.
[17] A.E. Blaurock, J. Mol. Biol. 56 (1971) 35–52.
[18] T.J. Torbet, M.H.F. Wilkins, J. Theor. Biol. 62 (1976) 447–458.
[19] W.C. Hung, F.Y. Chen, H.W. Huang, Biophys. J., submitted for publication.
[20] V. Luzzati, X-ray diffraction studies of lipid–water systems,

in: D. Chapman (Ed.), Biological Membranes, Academic Press, London, 1967, pp. 71–123.
[21] C.H. Hsieh, S.C. Sue, P.C. Lyu, W.G. Wu, Biophys. J. 73 (1997) 870–877.
[22] L.D. Landau, E.M. Lifshitz, Statistical Physics, Pergamon Press, New York, 1968, p. 256.
[23] S. Leikin, D.C. Rau, V.A. Parsegian, Phys. Rev. A 44 (1991) 5272–5278.
[24] D.M. Small, in: The Physical Chemistry of Lipids, Plenum Press, New York, 1986, pp. 475–522.
[25] G.S. Smith, E.B. Sirota, C.R. Safinya, N.A. Clark, Phys. Rev. Lett. 60 (1988) 813–816.
[26] R.H. Pearson, I. Pascher, Nature 281 (1979) 499–501.
[27] H. Hauser, I. Pascher, R.H. Pearson, S. Sundell, Biochim. Biophys. Acta 650 (1981) 21–51.
[28] T.J. McIntosh, S.A. Simon, Biochemistry 25 (1986) 4948–4952.
[29] J.F. Nagle, R. Zhang, S. Tristram-Nagle, W.-J. Sun, Biophys. J. 70 (1996) 1419–1431.
[30] A. Seelig, J. Seelig, Biochim. Biophys. Acta 406 (1975) 1–5.
[31] L. Yang, T.M. Weiss, T.A. Harroun, W.T. Heller, H.W. Huang, Biophys. J. 77 (1999) 2648–2656.
[32] G.S. Smith, E.B. Sirota, C.R. Safinya, R.J. Plano, N.A. Clark, J. Chem. Phys. 92 (1990) 4519–4529.